Noname manuscript No.
(will be inserted by the editor)

rSeiz 2.0: A Low Latency and Energy Efficient Seizure Detector in the IoMT

Md Abu Sayeed * · **Saraju P. Mohanty** · **Elias Kougianos**

the date of receipt and acceptance should be inserted later

Abstract Epilepsy affects 50 million people globally, which requires a real-time, low-power, and low-latency seizure detector to address the problem. An IoT-enabled real-time, energy-efficient, and fast seizure detector has been presented. The seizure detector consists of four crucial components: 1. Pulse Exclusion Mechanism (PEM) or neighborhood component analysis (NCA) for the selection of weighted channels, 2. Optimal feature extraction, 3. RBO optimized κ-nearest neighbor classifier for seizure detection, and 4. Internet of Medical Things (IoMT) for remote medi-cal services. The proposed system used two models for weighted channel selection: one uses PEM and the other uses NCA. Key features have been extracted from the weighted channels in a specified timing interval, and later, seizure detection is performed using RBO optimized κ-NN classifier. Both software and hardware validation were performed to evaluate the proposed approach. When PEM and RBO are used together, the system's latency is reduced dramatically while retaining optimal accuracy. The experimental results from software simulation and hardware implementation show that the proposed seizure detector outperforms the current state of the art and provides essential contributions to smart healthcare.

M. A. Sayeed (Corresponding Author)
Dept. of Mathematical Sciences., Eastern New Mexico University
E-mail: md.sayeed@enmu.edu.

S. P. Mohanty
Dept. of Computer Sci. and Eng., University of North Texas
E-mail: saraju.mohanty@unt.edu

E. Kougianos
Dept. of Electrical Engineering, University of North Texas
E-mail: elias.kougianos@unt.edu.

Keywords Internet-of-Medical-Things (IoMT) · Low-Latency · Energy Efficiency · Pulse Exclusion Mechanism (PEM) · channel reduction · EEG

1 Introduction

The traditional healthcare system is unable to accommodate the growing population [1,2]. IoT-enabled cutting-edge technologies for smart healthcare offer opportunities to enhance the current healthcare system and satisfy the demand of the increasing population [3]. The Internet of Medical Things (IoMT) is referred to a network of biomedical apps and equipment, is the basis of smart healthcare systems. Users of smart health care are empowered to handle some emergency circumstances on their own. It places a focus on enhancing the user's quality and experience. Utilizing the resources that are available to the maximum capacity is made possible by smart health care. One particular instance of smart healthcare is automated seizure detection.

Around 1% of people worldwide suffer from a chronic neurological condition known as epilepsy. Seizure is marked by loss of awareness, uncontrolled arm and leg movements, or convulsions [4–6]. Epileptics are unable to perform their daily tasks. For epileptic seizures to be diagnosed correctly and promptly, both the financial and human costs must be minimized. To treat epilepsy, antiepileptic drug (AED) has been widely used. Existing research found that Many epilepsy patients do not recover after taking medication, and AED is ineffective for drug-resistant patients. The recurrent seizures cause devastating effects on refractory patients, which hinder patients from doing daily activities. For patients who have failed treatment, surgery may be an alternative option. Surgery is not

a popular choice as it damages important brain areas for focal seizures [7,8]. Wearable and automated embedded devices are becoming an increasing need to treat biomedical diseases. An automated seizure detector can detect seizures with a minimum delay and provide an early warning so that prevention measures can be taken. Electroencephalography (EEG) is the representation of brain signals in terms of electrical waveforms. Electrodes are placed on different areas of the brain area as a cap that records electric voltage. EEG is effective in capturing brain dynamics that contain different psychological states [9]. Manual seizure detection through by visual inspection is costly and laborious, as the physicians require a significant amount of time to arrange the examinations for the epileptic subject and to monitor the patient's activity for an extended period of time [10].

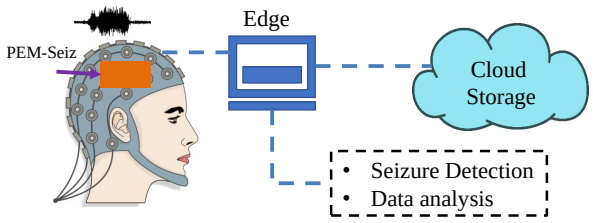

Fig. 1: Edge-IoMT module of the proposed rSeiz 2.0

In this paper, an RBO-based seizure identification approach has been presented that employs two different channel selection techniques: PEM and NCA. EEG data is tested for both channel selection techniques and the performance is evaluated. Real-time detection is performed with the stationary EEG data using a non-overlapping time frame. Time frames of different sizes have been adopted to evaluate accuracy and latency. Key features have been selected from the weighted channels using RBO. PEM-based features were applied to RBO optimized κ-NN classifier. Later, NCA-based features were fed to the classifier as well. The performance of the classifier is evaluated for both approaches and the resulting data is shown in the experimental results section. The module of the edge-IoMT framework is depicted on Fig. 1.

The contributions to the current state of the art are illustrated in section 2. The cutting-edge research in this area is discussed in Section 3. Section 5 conceptu-alizes the architecture and depicts different algorithms such as: PEM, NCA, feature extraction, RBO, and κ-NN classifier. Section 4 shows the implementation using software and hardware. The data from software simulation and hardware execution is described in Section 6. Section 7 briefly discusses potential ideas for future research and wraps up this paper.

2 Problem Statement and proposed Solution

2.1 Problem Statement

1. The existing research provides many seizure detection algorithms that mostly run on a desktop computer using recorded stationary data. Those algorithms analyze data and measure performance in terms of accuracy or similar parameters. The analysis of non-stationary data does not allow real-time detection. Automated and real-time solutions are becoming necessary to address epileptic seizures. How is it possible to detect seizures in real time? is a crucial research inquiry.

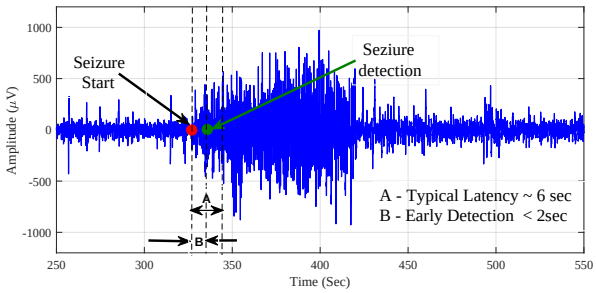

Fig. 2: Latency in seizure detection

2. A few seizure detection algorithms have been presented regarding latency, a crucial parameter for real-time seizure detection. The distance between the point at which a seizure starts and the time at which it is detected, called latency, is depicted in Fig. 2. The reported latency for the eisting algorithms is still high. The goal of biomedical research is to identify the problem and take appropriate actions if necessary. High detection accuracy is of no use if latency is high. A minimum latency alerts the designated user early so protective actions such as drug delivery or stimulation can be carried out immediately to halt the seizure progression. Another important parameter for wearable or implantable systems is power consumption, which directly affects device life. It is critical to minimize power consumption as the seizure detector requires complex circuitry that consumes more power. The earlier query is expanded to include the following question: How is real-time and energy-efficient seizure detection possible with minimal latency? This work

addressed those questions thoroughly and provided directions for future research.

2.2 Proposed Solution

In this work, PEM or NCA algorithm combines with RBO-based κ-NN to identify seizure onset in the IoT framework. The latency of the detector primarily depends on the length of the feature vector, processor speed, and data platform. Reducing the size of the vector will result in a decrease in computational time. Incorporating PEM and RBO reduces the feature vector's size in two steps. In the first step, PEM examines each EEG channel, keeping only the channels with a high weight. In the second step, less important features are cut down using RBO. The shrink in the size of the feature vector leads to faster training and testing of the classifier, hence reducing the latency of the detector. PEM also uses a small set of functions that require low time for computation. The training is conducted offline; the training time or huge dataset barely affects the delay of the detector. The type of data platform also affects the latency. While cloud IoMT performs data analysis on the cloud, edge IoMT performs data com-putation at the sensor node. The computation in the edge-IoMT provides a significant reduction in latency compared to the computation performed on edge-IoMT [11]. Wearable or implantable medical devices need en-ergy efficiency as battery life is a pivotal factor. It is not feasible to replace the battery often. The implementation of PEM function requires fewer components with simple circuitry. The other functions also fulfill the low-power requirement. A pattern-independent black box-based approach is used to measure power consumption. The use of minimal circuitry associated with the system leads to a reduction in power consumption.

2.3 Novel Contributions of This Work

1. Most of the existing seizure detection systems are patient-specific and are not effective for new epileptic subjects. The proposed approach tests the new raw EEG data in real-time. The proposed model utilizes an extensive and diverse training dataset that encompasses samples from a wide range of patients. By incorporating a diverse patient population, including those with unknown identities or distinct characteristics, this approach acquires more generalized patterns and accommodates individual dissimilarities.
2. Smart healthcare systems require low latency automated devices for fast seizure detection. The length of the feature vector is a crucial factor that constitutes latency of the system. The proposed PEM leads to a 70% reduction in the number of channels. The RBO optimization shrinks the feature's size. As a result, the length of the feature vector both in the training phase and testing phase decreased significantly. The feature vector length has a proportional relationship with the detection latency. The decrease in vector length eventually reduces the delay of the seizure detection system.
3. Seizure control through drug delivery or stimulation processes requires minimal false detection for practical epilepsy solutions. The proposed PEM-based classifier captures non-seizure patterns effectively and eliminates noises and redundant pulses associated with EEG signals which leads to a sharp decrease in false detections. The proposed method outperforms the current state-of-the-art in terms of latency, power consumption, and accuracy.

3 Related previous research

A patient-specific seizure detection technique [12] is presented that forms a machine-learning framework using a support vector machine. It identifies the crucial features that distinguish seizure characteristics from other psychological signals. The validation of this approach with a non-invasive EEG dataset provides accuracy and latency of 96% and 4.6 sec, respectively. A signal rejection algorithm (SRA) [13] is employed to improve the performance of the detector. The combination of a voltage level detector and SRA is proven to be very useful in capturing EEG dynamics and distinguishing different patterns of EEG signals. It reports an improved accuracy of 96.9%. A low-power seizure detector [14] is introduced that uses Hjorth parameters to distinguish different EEG signals and deep neural networks (DNN) to assign the features in a different class. It is evaluated in the icEEG Bonn dataset. The proposed seizure detector consumes less power which may be useful for wearable devices. The seizure detector is perceived on the IoT edge to enable remote healthcare monitoring and treatment. It is noticed that edge IoT reduces the latency with respect to the existing state of the art.

An algorithm has been developed [15] that uses BRRM recurrence biomarkers and ONASNet network. BRRM represents non-linear dynamics of the complex EEG signals. Transfer learning is employed in the ONASNet architecture for EEG data analysis. The use of both BRRM and ONASNet enables features to be extracted from different brain zones. Data labeling-based

approach [16] is presented, which overcomes the complexity issue with manual data labeling. It uses unsupervised learning (UL) for data labeling. The enhanced classification of the indeterminate subjects is carried out using the Unsupervised learning (SL) approach. It is the first time UL and SL have been integrated for seizure detection. A New Neural Mass (NNM) [17] is presented in which dynamic features of the epileptic EEG can be characterized from the model's parameter. Later, DF method was applied for early seizure detection. The NNM-based approach provides 100% sensitivity and a latency of 7.1 sec. A system [18] is proposed that combines RDCSAE stack autoencoder and IKRVFLN network to capture seizure characteristics using single and multi-channels. RDCSAE analyzes EEG signals and extracts unsupervised features which are fed to IKRVFLN classifier for training. Efficient training is conducted by adjusting the cost function and this approach reports a high classification accuracy.

A robust method [19] is presented for seizure detection using a complex deep neural network (CDNN) model and Adversarial Representation Learning (ARL). The CDNN model captures seizure and non-seizure EEG dynamics through Adversarial Learning. This approach was evaluated using TUH EEG dataset and the results show that it reduces latency considerably. A unified model [9] is developed for epileptic seizure detection that combines both the spectral and temporal domain and resolves the issue with existing deep learning models. It was evaluated using three different datasets: CHIB MIT Scalp, Bonn, and TUSZ dataset. An intracortical microelectrode array (MEA) [20] signals have been introduced first time for early detection of human epileptic seizures. It uses nonlinear support vector machines (SVMs) for distinguishing seizure and non-seizure characteristics. Intracortical MEAs may be useful for synchronous seizure control. An efficient technique [21] for seizure detection is presented that uses Stockwell transform (S-transform) for obtaining time-frequency blocks and bidirectional long short-term memory (BiLSTM) for classification. The postprocessing of the EEG signals provides enhanced detection performance.

A hybrid seizure detection method [22] is proposed that utilizes both cEEG and aEEG. The cEEG based approach divides EEG signals into 5 sec time frame with a 4-sec overlap, and the feature vector was applied to the random forest classifier for seizure detection. On the otherhand, aEEG is used for spike detection. Movement-based approach [23] uses Passive InfraRed (PIR) sensors to capture human body movement during sleep. Body movement during an epileptic seizure is different from ordinary sleep. Machine learning algorithms have been used to identify different body movement patterns. Data from the PIR sensor is fed to hidden Markov model (HMM) and convolutional neural network for classification. An accurate method for non-convulsive seizure detection [24] has been developed. It uses LDA, RBSVM, and k-NN algorithm for feature classification. Hilbert-Huang transform (HHT) is used to expand the EEG. The scalp EEG dataset is utilized to evaluate performance. The proposed method provides accuracy, a true positive rate, and a true negative rate of more than 98%.

In our previous work, a rapid seizure detection method [25] was presented that uses a limited dataset. The method requires the validation of extensive data. This work has extensively validated two widely available EEG datasets, including software simulation and hardware implementation. This paper uses a novel PEM in combination with RBO, which drastically reduces the latency of the system.

4 The Proposed Seizure Detection Approach

Proposed system mainly have four parts: 1. time frame formation 2. Pulse Exclusion Mechanism (PEM) or Neighborhood Component Feature Selection (NCFS) for channel selection 3. Statistical Feature Extraction 4. Relif based optimazed κ-NN classifier. Fig. 3 and Fig. 4 illustrate the proposed system's architecture and flowchart, respectively.

4.1 Time Frame Formation

One of the crucial points of real-time seizure identification is the selection of the size of the time frame. The possibility of accurate detection increases with increasing the size of the time frame, as a bigger timing window contains enough samples to represent normal and abnormal EEG patterns over time. But it increases latency in seizure detection. A low-sized time frame reduces the delay of the system, but it decreases the accuracy. Both accuracy and power consumption are pivotal factors for low latency and energy-efficient biomedical applications. This experiment is conducted for varying time frames (3-sec, 6-sec, and 9-sec) and results are recorded. At a 256 Hz sampling rate, the following time frames, 3-sec, 6-sec, and 9-sec, contain 768, 1536, and 2304 samples, respectively. Each time frame consists of three non-overlapping segments. For example, a combination of three non-overlapping segments of 1-sec constitutes a 3-sec frame, whereas the 3-sec non-overlapping segment creates a 9-sec frame.

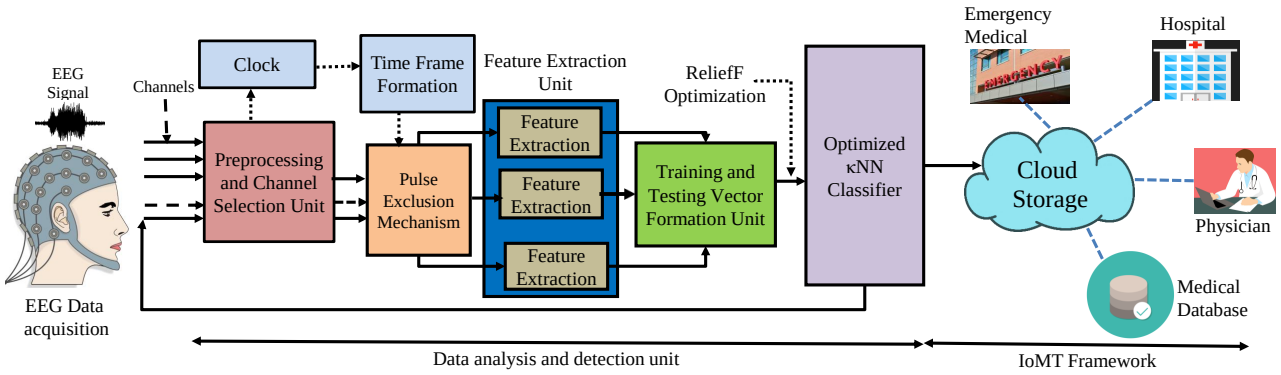

Fig. 3: Architecture of the proposed PEM-Seiz

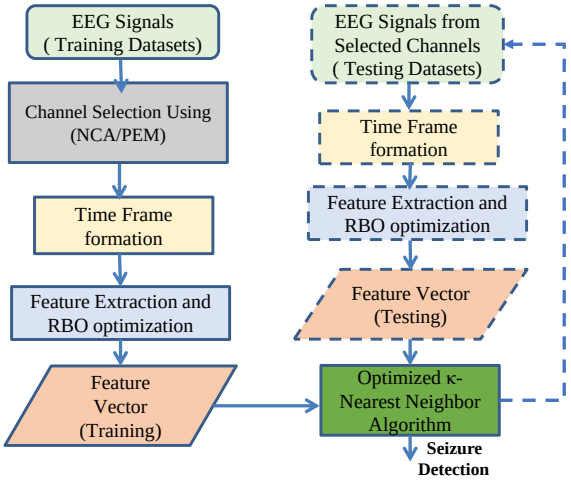

Fig. 4: Proposed algorithm for seizure detection

The 3-sec frame overlapped by the next frame by 2-sec. The 6-sec and 9-sec frames are overlapped by 5-sec and 8-sec, respectively, as indicated by Table 1. The moulding of the time frame on the EEG signal at the designated length is depicted in Fig. 5 and Fig. 6.

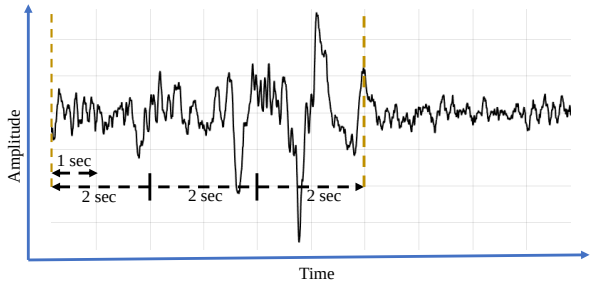

Fig. 5: Illustration of the time frame formation for 6-sec window

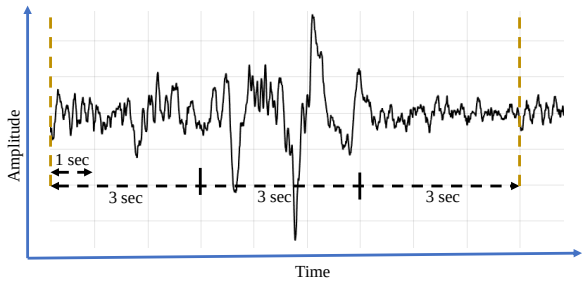

Fig. 6: Time frame structure of 9-sec window

Table 1: Time Frame Data

Frame size in Time	Number of Samples	Length of the overlapping segments	Length of the Non-overlapping segments
3 sec	768	1 sec	2 sec
6 sec	1536	2 sec	5 sec
9 sec	2304	3 sec	8 sec

4.2 Pulse Exclusion Mechanism (PEM) for channel selection

PEM is proven to be an effective approach to reduce heavy computation by removing insignificant attributes. PEM analyzes each time frame and places 1 or 0 on the time frame according to different EEG activities. If the time frame is closer or within the ictal area, PEM inclines to place 1. If the time frame is within the non-seizure area, PEM tends to place 0. During seizure activities, there is a large number of 1's and a small number of 0's in the time frame. On the otherhand, during non-seizure activities, 0 become dominant. The idea is to distinguish seizure and non-seizure behavior by simply calculating number of 1's or 0's in the time frame. The distinction between seizure and non-seizure characteristics are evident for some channels. PEM algorithm

analyzes EEG data and determine the channels with high weight value.

The creation of 0's can be expressed as:

$$A(n) = \begin{cases} 0, & A(k-5) = 0 \text{ or } A(k-4) = 0 \\ & \text{or } A(k-3) = 0, \text{ if } A(k-2) = 0 \\ 0, & \text{otherwise.} \end{cases} \quad (1)$$

The creation of 1's is expressed as:

$$A(n) = \begin{cases} 1, & A(k-5) = 1 \text{ and } A(k-4) = 1 \\ & \text{and } A(k-3) = 1, \text{ if } A(k-2) = 0 \\ 0, & \text{otherwise.} \end{cases} \quad (2)$$

4.3 Neighborhood Component Feature Selection (NCFS) for channel selection

The computation time and delay will be large if feature extraction is applied to all EEG channels. It would be beneficial to choose the right number of channels that could offer fast and accurate detection. Assume that N samples of EEG signals constitute a training set T which contain normal EEG, ictal activities, and interictal activities:

$$T = (F_u, f_u), U = 1, 2, ...N \quad (3)$$

where F_u and f_u represent feature vector and corresponding class labels, respectively.

The objective is to compute feature weight that maximizes the classification of the nearest neighbor. The distance between a given instance and its nearest neighbor is expressed by the feature weight using the following expression [26]:

$$D_w(F_u, F_v) = \sum_{q=1}^{d} {w_q}^2 |F_{uq} - F_{vq}| \quad (4)$$

where w_q is the qth channel's weight. An effective strategy is to improve the performance of the nearest neighbor classification by maximizing leave-one-out detection accuracy. For selecting the reference point, the probabilistic distribution function is employed. The possibility of the selection A is [26]:

$$P_{uv} = \begin{cases} \frac{k(D_w(F_u,F_v))}{\sum_{k \neq u} k(D_w(F_u,F_v))}, & \text{if } u \neq v \\ 0, & \text{if } u = v \end{cases} \quad (5)$$

The probability that F_u will be appropriately identified as a seizure or not.

$$p_u = \sum_{v} b_{uv} p_{uv} \quad (6)$$

The leave-one-out classification accuracy can be expressed using the following expression:

$$\epsilon(w) = \frac{1}{N} \sum_{u} p_u = \frac{1}{N} \sum_{v} \sum_{v} b_{uv} p_{uv} \quad (7)$$

A regularization parameter termed λ is introduced to reduce over-fitting, resulting in the following function:

$$\epsilon(w) = \sum_{v} \sum_{v} b_{uv} p_{uv} \qquad - \lambda \sum_{q=1}^{d} {w_q}^2 \quad (8)$$

4.4 Statistical Feature Extraction

To capture non-stationary and complex EEG dynamics, the statistical parameters variance, activity, and signal complexity are useful [27]. These parameters enable measurement of the degree of variations along a signal. While signal complexity considers second-order changes, signal mobility covers first-order variations. Take into account an EEG signal Y_p with $p = 1, 2, 3, 4, 5, 6..., N$. The signal a_q is the first order variations in y with $q = 1, 2, ...N - 1$.

$$a_q = y_{q+1} - y_q \quad (9)$$

b_r is the second order variants in y with $r = 1, 2, ...N-2$

$$b_r = a_{r+1} - a_r \quad (10)$$

$$\text{Activity} = \sqrt{\frac{\sum_{p=1}^{N} (y_p - mean)^2}{N}} \quad (11)$$

$$V_0 = \sqrt{\frac{\sum_{p=1}^{N} (y_p)^2}{N}} \quad (12)$$

$$V_1 = \sqrt{\frac{\sum_{q=2}^{N-1} (a_q)^2}{N-1}} \quad (13)$$

$$V_2 = \sqrt{\frac{\sum_{r=3}^{N-2} (b_r)^2}{N-2}} \quad (14)$$

The expression for signal complexity (SC) and signal mobility (SM) can be obtained as follows:

$$\text{Signal Mobility} = \frac{V_1}{V_2} \quad (15)$$

$$\text{Signal Complexity} = \sqrt{\frac{V_2^2}{V_1^2} - \frac{V_1^2}{V_0^2}} \quad (16)$$

4.5 Relif based optimized κ-NN classifier

The key to the Relif principle is to assign a weight to the attributes that evaluate their usefulness. Relif looks for its closest neighbors in both the same class and in a different class for a random instance [28]. The closest hit is the same class, while the closest miss is a different class. The weight of the attributes has been estimated based on the hit, miss, and random instances. If the instance and hit have different values, then the value of the weight decreases. If the instance and miss have different values, then the value of the weight increases [29]. The originally proposed Relif algorithm cannot deal with classification problems that have more than two classes. That algorithm was later extended to ReliefF, which solves multiclass problems effectively. ReliefF chooses an instance at random and then looks for κ of its nearest neighbors in the closest hit and closest miss. Based on the hit, miss, and random cases, the weight of the attributes has been assessed. The expression for RelifF algorithm follows Relief algorithm with the exception of averaging the contributions from all hits and all misses. The prior probability of the class weighs the input for each class of misses (C). In each step, tits or misses should be in the range of [0,1], and it needs to ensure that probability weights for misses add up to 1.

In the ReliefF algorithm, each feature is ranked according to its weight and the removal of insignificant features reduces the computation time of the classifier. Assume that the set of weights AW1, AW2,..... AWn belongs to the following features A1, A2, ... An. The update of the weight is conducted iteratively, and initially, the weight values have all been set to 0. The algorithm chooses z_u and locates its closest instances. Then, for each of these neighbors, referred to as z_v, all the weights are adjusted. The following expression calculates the score of a certain feature A_j at the ith iteration if the random instance and the nearest neighbor are in the same class [30].

$$AW_j{}^i = AW_j{}^{i-1} - \frac{\Delta_j(x_s, x_t)}{q_{EEG}} * d_{st} \tag{17}$$

If the random instance and the nearest neighbor are in a different class, the weight importance can be determined by the following expression.

$$AW_j{}^i = AW_j{}^{i-1} - \frac{p_{y_t}}{1 - p_{y_s}} \frac{\Delta_(x_s, x_t)}{m_{EEG}} * d_{st} \tag{18}$$

The distance function is given by d_{st}. p_{y_t} and p_{y_s} stand for the class's prior probability, to which a random instance or nearest neighbor belongs, respectively. For the nearest neighbor or random instance, the difference in extracted features is defined as [30]:

$$\Delta_(x_s, x_t) = \frac{|x_{sj} - x_{tj}|}{max(A_j) - min(A_j)} \tag{19}$$

The training stage and the testing stage make up the two phases of the κ-NN algorithm [31]. The training step includes the storage of training vectors from the ReliefF-based optimization (RBO) and class labels. In real-time classification, the classifier is given a query point to test, this algorithm decides who are the closest neighbors, and the query point is given a class by a vote among the neighbors. The value of κ and the distance metric have been adjusted to achieve maximum classification accuracy. A high value of κ is effective in removing noises from the EEG signals but it reduces the accuracy of the classifier. The value of κ is adjusted, which is a tradeoff between accuracy and noise. The Euclidean distance between P(p1, p2, p3,..., pn) and Q(q1, q2, q3,..., qn) in the vector space can be expressed as:

$$d_{EEG}(p, q) = \sqrt{\sum_{i=1}^{n} (p_i - q_i)^2} \tag{20}$$

5 Software simulation and Hardware Implementation

Fig. 7 shows the system-level diagram of the proposed system. Signals were imported to the MATLAB workspace and then submitted to NCA or PEM algorithm. The structure of the NCA and PEM algorithms has been constructed using Simulink user-defined functions. These algorithms extracted the key channels. The EEG signals with reduced channels were applied to the RelifF based optimization (RBO) for feature reduction. RBO is cre-ated in the diagram by another user-defined function. The reduced feature vectors from the specified time frame were continuously fed to the κ-NN classifier. The training was performed for a significant amount of time for the MIT-Scalp dataset. The short-duration Bonn dataset was trained quickly as it contains fewer sam-ples. The overall latency of the system is not much af-fected by the training time as the training is performed offline. Testing time and testing vectors constitute the major portion of the delay. Latency depends on the size of the feature vectors and other parameters of the system-level simulator.

A crucial performance parameter for wearable or implantable sensors is power consumption, which should be kept as low as possible to enhance battery life. The

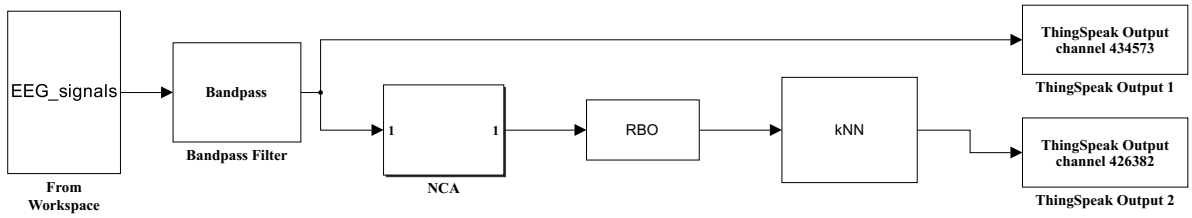

Fig. 7: Proposed system in the system level simulator

computation of power consumption is performed using an approach that is independent of the pattern. In this approach, the detector is simulated several times with varying input EEG signals. Power consumption is recorded for each input EEG signal. The data were then averaged to obtain the real power consumption. Simscape power-measurement circuitry is added to the system to compute the power consumption. It requires a Simulink-PS converter unit that connects the proposed seizure detection system to the Simscape network. The Simscape network includes the components: current sensor, voltage sensor, voltage source, and current source. A PS- Simulink converter connects Simscape output to a Simulink block. The voltage and current sensor deliver the voltage and current data, which evaluates the system's total power consumption. Power is estimated for both icEEG (Bonn dataset) and scalp EEG (MiT Scalp EEG database) for varying patients. The reported power consumption is almost identical irrespective of the epileptic subjects. For example, the power consumption of chb01 is measured as 66.23 μw, whereas chb03 reports 65.85 μw.

The proposed system is prototyped with Arduino UNO board using HIL(hardware-in-loop) based technique. The LCD and Arduino UNO board are the necessary parts for implementation. The Arduino UNO board can be interfaced with other sensors or circuits, enabling its application in many projects. In addition to 32 KB of flash memory, it contains 2 KB of static random-access memory (SRAM). There is also a 1 KB EEPROM integrated. The Arduino board includes 14 digital pins, numbered [0–13], and six of these can be used for pulse width modulation (PWM). It has six analog pins: [A0-A5] that can read and write analog data using external sensors. The DC current for each pin is 20 milliamps (mA). IoT devices require data transmission through Arduino board or external devices. Data transmission is a key requirement for the implementation of the IoT devices. Pin 1 (Tx) and pin 0 (Rx) allow data to be transmitted and received from the board to the external devices and vice versa. The data from the board can be displayed on the serial monitor associated with Arduino IDE software. A vendor-provided package was utilized to build and configure the system-level simulator.The proposed system is prototyped in Fig. 8.

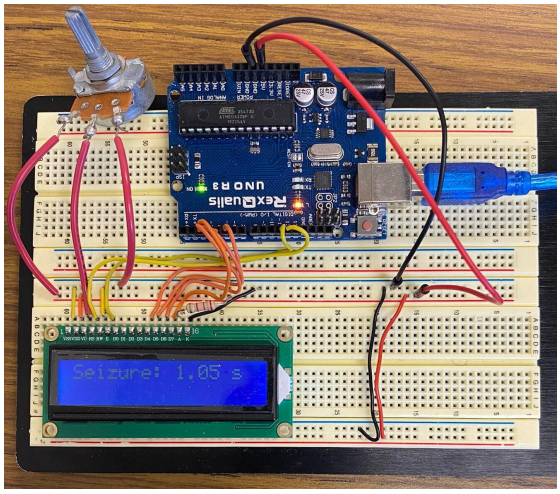

Fig. 8: Breadboard set-up and implementation

Patient's healthcare data and seizure-related information is displayed on the liquid crystal display (LCD). The formation of the display can be controlled by manipulating the interface pins. The interface is comprised of the following pins: RS, R/W, E, D0-D7, V0, VSS, VDD, and LED backlight (A. K). RS pin controls whether the data or instruction is sent to the LCD. If RS is set to 0, a command is sent to LCD. The data is sent to the LCD if RS is set to 1. R/W pin selects whether to read or write to the LCD. A pin labeled "E" permits writing to registers. The data pins from D0 to D7 allowed 8 bits of data to be written to the register. A potentiometer is attached to the V0 pin to control the contrast of the LCD screen. VSS and VDD are power supply pins connected to ground and +5V, respectively. A and K pins are used to control the LED backlight. ThingSpeak, which is an open data platform, implemented IoMT devices. The EEG channel and seizure channel were created in ThingSpeak. EEG recordings of patients were

preserved in the EEG channel, whereas seizure recordings and useful information were only kept on the seizure channel.

6 Experimental Results

The proposed seizure detector was validated with two widely used databases, which have been discussed below.

6.1 Validation With Bonn Dataset

The proposed system was initially validated with short-duration EEG datasets obtained from the following source [32]. The data sets A, D, and E were used for the evaluation. The data is sampled at 173.61 Hz frequency. Each dataset is subdivided into 100 EEG segments, and 4097 samples are assigned for each segment. Dataset A represents the EEG recording from normal EEG, whereas D is the EEG recording during interictal states. The ictal activities were stored in dataset E. Fig. 9a shows the waveforms for different EEG states. The feature values have been computed from all the epochs, and the results show that the feature value of the ictal epoch differs from the feature value obtained from the normal or interictal epoch. Fig. 9b shows the SM values for eight EEG epochs. For epoch 1, the SM value is reported as 0.3 for normal EEG. For ictal EEG, the SM value becomes 0.34. For EEG sample 8, the SM value for normal and ictal EEG becomes 0.29 and 0.34, respectively. There is always a distinction between normal EEG and ictal EEG.

The extracted features form the feature vectors. The length of the vector is linearly dependent on the number of features and non-EEG epochs. Each time frame consists of 3 X 3 X 1 = 9 elements. Features are continuously trained using an RBO-based κ-NN classifier. To train the classifier, 80% of each dataset was used, while the remaining 20% was allocated to testing. The training data includes a total of 240 EEG epochs, and testing data involves 60 EEG epochs from datasets A, D, and E. The testing was performed in two different cases: normal EEG (A) VS ictal EEG (E) and normal and interictal EEG (AD) VS ictal EEG (E).

Both the system's performance with regard to its individual features and its combination of features was assessed. For normal EEG (A) VS ictal EEG (E), the proposed approach reports a 100% sensitivity and 100% specificity for single or combined features. For normal and interictal EEG (AD) VS ictal EEG (E), it reports an average of 97.6% sensitivity for individual feature SM and 98.5% sensitivity for SC. However, the combination of SC and SM provides 100% sensitivity and 100% specificity. Table 2 shows comparative data for the Bonn dataset. The detection latency is negligible as the Bonn dataset is short durations and does not contain enough samples. The data relating to latency is discussed in the next section for CHB-MIT scalp dataset.

Table 2: Evaluation of the proposed approach for Bonn dataset

Reference	Details of the Method	Sensitivity (%)	Specificity (%)
Olokodana, et al. (2020) [33]	DWT, FD and kriging model	100	100
Sayeed, et al. (2019) [14]	DNN - Hjorth parameters	100	96.9
Dauod, et al. (2018) [34]	EMD, feature extraction	100	98
Wen, et al. (2017) [35]	GA with kNN classifier	100	98
Sayeed et al. (2023)[current paper]	PEM and RBO optimized kNN	100	100

6.2 Validation With CHB-MIT Scalp Dataset

The EEG data from CHB-MIT [36] is chosen for validation purposes. The patient's age, gender, and seizure information are listed in Table 3. It includes two male and eight female subjects. Epileptic subjects 1 (chb01) and 3 (chb03) have seven seizures each, and both chb05 and chb08 hold 5 seizures. The remaining epileptic subjects (chb02, chb07, chb11, chb17, and chb19) record 3 seizures each.

Table 3: Epileptic Patient's information

Patient's Order	File Name	Patient's Gender and age	Number of seizures
1	chb01	Female - 11 years	7
2	chb02	Male - 11 years	3
3	chb03	Female - 14 years	7
4	chb05	Female - 7 years	5
5	chb07	Female - 14.5 years	3
6	chb08	Male - 3.05 years	5
7	chb09	Female - 10 years	4
8	chb11	Female - 12 years	3
9	chb17	Female - 12 years	3
10	chb19	Female - 19 years	3

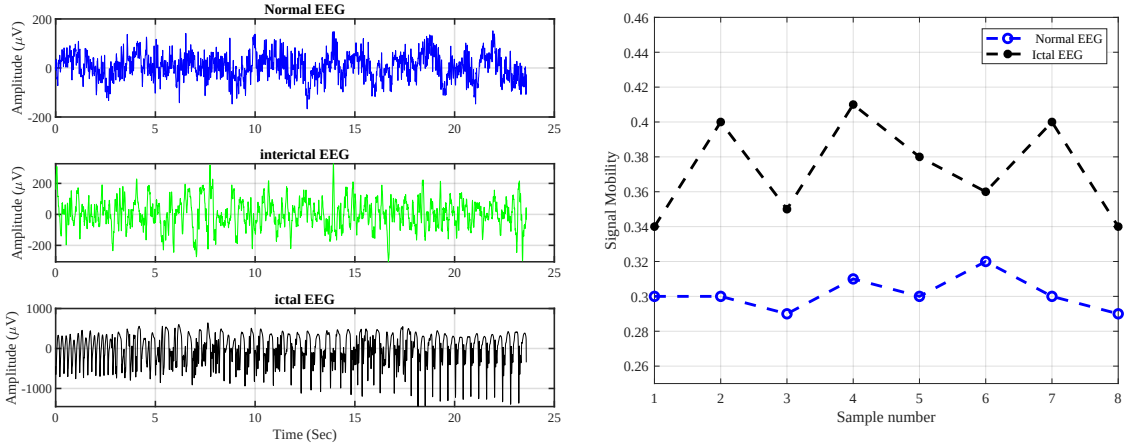

(a) (b)

Fig. 9: (a) Depiction of normal (TOP), interictal (middle), and ictal EEG (left) (b) Variation of signal mobility for icEEG

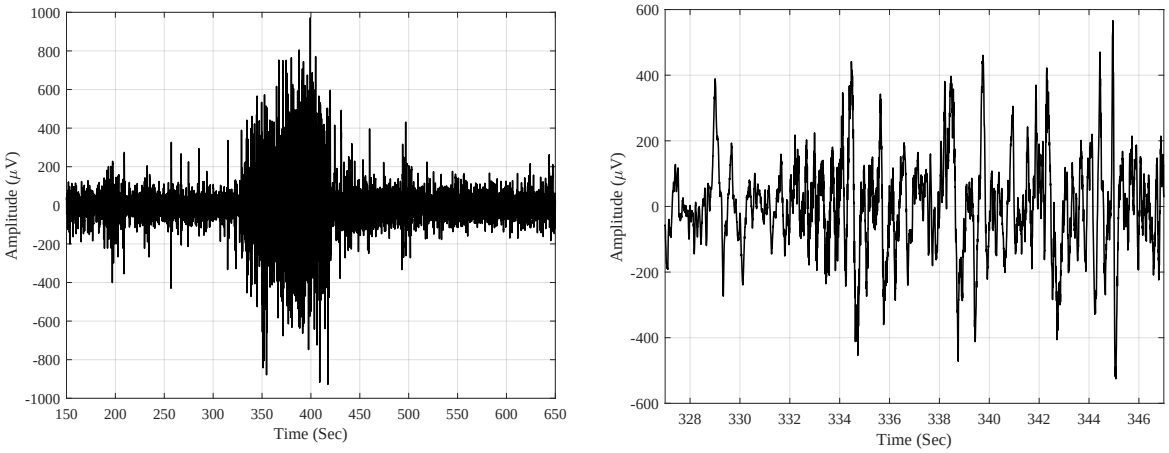

(a) (b)

Fig. 10: Transient analysis (a) EEG signals (150 sec - 650 sec) from epileptic subject chb01 (b) seizure activities (327-347 sec)

Fig 10 shows the transient analysis of a scalp EEG waveform of a particular epileptic subject chb01. For chb01 subject, seizure activity starts at 327 sec and ends at 420 sec. At a 256 Hz sampling frequency, seizure activities span the samples between 83,712 and 107,520. The amplitude of the samples is less than 300 μV before the seizure onset point. The amplitude level rises to 800 μV during the seizure activity, which stipulates that seizure onset is associated with a high amplitude discharge. A bandpass filter is used to filter out unwanted pulses and erroneous detections from EEG signals. Filtered signals contain EEG signals from 23 channels, which are applied to NCA to eliminate insignificant channels. The regularization parameter λ is patient-specific and varies for different subjects. 10-fold cross-validation is performed to determine the best λ value. NCA analyzes and retains high-weighted channels whose weight values exceed a certain threshold point. The channel's retention or elimination following the application of NCA is shown in Table 4.

NCA only keeps eight channels out of 23 channels. Another approach that is adopted to eliminate less-weighted channels is PEM. PEM algorithm is employed to retain high-weighted channels by distinguishing non-seizure and ictal pulses from EEG signals. A seizure leads to a high-amplitude discharge (also called hyper-synchronous discharge) in the onset area of a particular frequency limit. Because of the high magnitude discharge during ictal activities, the samples in seizure-prone areas contain a higher number of 1's. On the

Table 4: channel's retention or elimination based on NCA

Channel No.	Channel Name	NCA Output
i	FP1-F7	eliminated
ii	F7-T7	retained
iii	T7-P7	eliminated
iv	P7-O1	retained
v	FP1-F3	retained
vi	F3-C3	eliminated
vii	C3-P3	eliminated
viii	P3-O1	eliminated
ix	FP2-F4	eliminated
x	F4-C4	eliminated
xi	C4-P4	eliminated
xii	P4-O2	eliminated
xiii	FP2-F8	retained
xiv	F8-T8	retained
xv	T8-P8	eliminated
xvi	P8-O2	eliminated
xvii	FZ-CZ	retained
xviii	CZ-PZ	eliminated
xix	P7-T7	eliminated
xx	T7-FT9	retained
xxi	FT9-FT10	retained
xxii	FT10-T8	eliminated
xxiii	T8-P8	eliminated

contrary, the non-seizure area holds a higher number of 0's as low amplitude pulses dominate the normal EEG area.1 indicates pulses that surpass the amplitude threshold of the epileptic subject. On the other hand, 0 indicates that those pulses are below the threshold level. The amplitude threshold captures the hypersynchronous discharge and gives a similarity in a particular EEG segment. PEM analyzes the channels and sets the amplitudes of most samples to 1 for the EEG segment with seizure activities. PEMS sets the amplitudes to 0 for the EEG segment with non-seizure activities. PEM sets a particular sample to 1 if 1 is dominant on the EEG segment. If 0 is dominant on that segment, PEM sets the sample 0. Some human behaviors, such as stress, sneezing, or emotion, may produce samples of amplitude similar to hypersynchronous pulses and give rise to false detections. PEM algorithm is embedded with a frequency span of 0 to 30 HZ to resolve the drawback of false detections.

An illustration of creating 0's and 1's in a particular EEG segment of eight samples is depicted in Table 5. The output waveform from the filter is analyzed to describe the PEM mechanism. Consider eight samples from non-seizure and seizure areas each. Ictal areas hold a higher number of 1's because of hypersynchronous discharge. The samples at the non-seizure areas are 01010001, which includes three 1's and five 0's. PEM reduces the number of 1's during 1st and 2nd execution. The non-seizure area becomes 00000001 at the end of the execution. On the other hand, 11011010 represents seizure activities. PEM increases the number of 1's in each execution, and the two executions make seizure area 11111110. The transient analysis of PEM signals have been depicted on Fig. 11.

Table 5: Application of PEM on seizure and non-seizure area

EEG location	Non-seizure area	Seizure area
1	0 1 0 1 0 0 0 1	1 1 0 1 1 0 1 0
2	0 1 0 0 0 0 0 1	1 1 1 1 1 0 1 0
3	0 0 0 0 0 0 0 1	1 1 1 1 1 1 1 0

Table 6: Feature vectors for signal mobility (SM)

Feature No.	Channel No.	Normal EEG	ictal EEG
1	10	0.1833	0.5820
2	10	0.1613	0.7418
3	10	0.1571	0.6651
4	10	0.2059	0.6557
5	10	0.2243	0.5662
6	10	0.1870	0.7789
7	10	0.2011	0.7632
8	10	0.2297	0.4857
9	10	0.2285	0.4386
10	10	0.1723	0.5703

EEG signals were applied to the feature extraction, and the extracted features formed feature vectors for a specified time frame. The length of the feature vector can be obtained by multiplying the number of features (Q = 3), the number of channels (N=8), and the number of non-overlapping EEG epochs (P=3). In each time frame, the feature vector has 8 x 3 x 3 = 72 elements. NCA or PEM leads to a 70% reduction in channels, reducing the computational burden. The feature vectors were then fed to RBO. RBO uses a ranking system and ranks the elements. The elements with rank [1-20] were considered, and the remaining elements [21-72] were removed. Later, the updated feature vectors from RBO were submitted to the κ-NN classifier. Two hours of normal EEG recording and 5 hours of interictal EEG recordings were employed for training. To train the seizure instances, a Z-1 number of instances have been used for Z seizures. 1 is labeled as seizure, and 0 represents non-seizure. The data is trained offline using feature vectors from the time frames, requiring significant training time. In the detection phase, the continu-

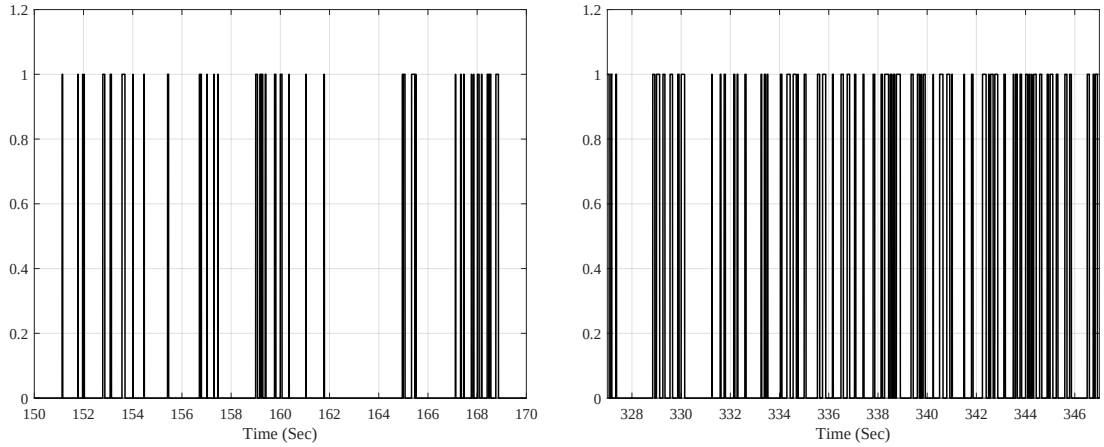

(a) (b)

Fig. 11: Transient analysis (a) normal EEG activities of time span 150-170 sec (b) seizure activities of time span 327- 345 sec

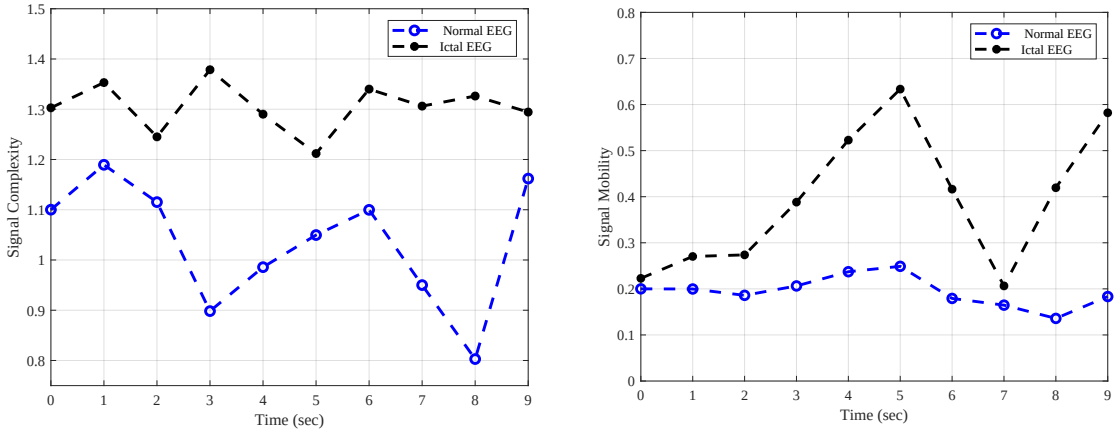

(a) (b)

Fig. 12: Variation of feature values with time (a) Signal complexity (b) Signal mobility

ous EEG samples constitute the testing vectors, which were tested for seizure detection. The sensitivity and latency were computed for different time frames. 3-sec time frame provides an average delay of 0.7 sec, but it reports a sensitivity of less than 80%. The low-sized time frame (3 sec) does not contain enough samples to correctly identify seizure progression over a while. The latency is low as it can quickly move to the next non-overlapping epoch. On the other hand, a high-sized time frame (9 sec) can be more effective in capturing seizure progression, which leads to better sensitivity. The drawback is that the delay is higher as the distance to the next EEG segment is high. A medium-length time frame (6 sec) overcomes the issue with sensitivity and latency, and provides the best performance.

Fig. 12 shows the progression of signal complexity (SC) and signal mobility (SM) over time. At t= 0 sec, the SC value for normal and ictal EEG are 1.1 and 1.3, respectively. At t=20 sec, the values become 1.16 for normal EEG and 1.29 for ictal EEG. SM values are initially 0.2 and 0.22 for normal and ictal EEG when t = 0 sec. SM values become 0.58 and 0.19 when t = 20 sec. SC and SM values are higher in ictal EEG than the normal EEG. This characteristic is employed to distinguish seizure instances from EEG signals. Table 6 shows feature values for a specific channel 10. The detection latency of each epileptic subject is depicted in Fig. 13.

The average overall latency is computed as 1.05 sec when PEM is used for channel selection, and RBO is utilized for feature reduction. The utilization of NCA and RBO leads to an increase in latency of 1.49 sec. Epileptic subject chb03 reports the lowest latency of

Table 7: Evaluation of the proposed system with current state of the art

Reference	Details of the Technique	Latency (sec)	Sensitivity (%)	Specificity (%)	IoT Framework
Vidyaratne, et al. (2017)[37]	Self similarity based FD, harmonic wavelet packet transform (HWPT), and Relevance vector machine (RVM) for robust classification	1.89	96	0.1/hour	NA
Aldana, et al. (2019) [24]	EEG expansion using Hilbert-Huang transform(HHT), LDA, RBSVM,and k-NN classifier for feature classification	NA	98	98	NA
Wu, et al. (2019) [22]	cEEG and aEEG based hybrid technique, feature extraction, and Random forest classifier	NA	99.41	82.98	NA
Fan, et al. (2019) [38]	Captures recurrence pattern of EEG using temporal synchronization and feature extraction, control chart to track the transit	6	98	NA	NA
Sayeed, et al. (2019) [13]	Level detection algorithm to analyze overexcited neurons and Pulse elimination algorithm for real time seizure detection and	3.6	96.9	97.5	Yes
Li, et al. (2020) [9]	uses temporal and spectral features and CEstSENet excitation network to distinguish seizure characteristics	1.39	2.41	96.05	NA
Olokodana, et al. (2020) [33]	Discrete wavelet transform (DWT) based fractal dimension feature extraction, and kriging model for feature classification	0.85	87.6	NA	Yes
Song, et al. (2020)[17]	New neural mass (NNM) for epileptic EEG characterization from dynamic features, DF method to detect seizure early	7.1	100	NA	NA
Peng, et al. (2021) [39]	Homotopy (DLWH) based Dictionary Learning and sparse representation based on an EEG training sample	NA	95.38	94.33	NA
Guo, et al. (2022) [16]	Integration of unsupervised learning (UL) for data labelling and supervised learning (SL) for seizure classification	NA	95.55	92.57	NA
Sayeed et al.(2023)[current paper]	Pulse exclusion mechanism (PEM), NCA(Neighborhood component analysis), and RBO optimized kNN classifier	1.05	97.6	100	Yes

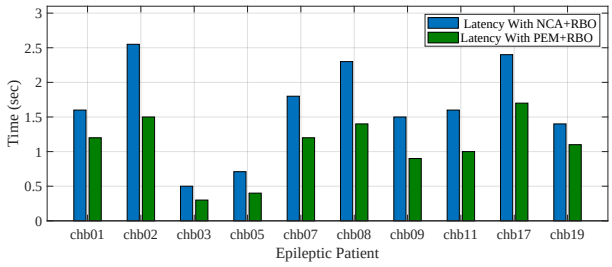

Fig. 13: Average latency for each epileptic subject

0.3 Sec (PEM+RBO), and chb02 provides the highest delay of 2.5 sec (NCA+RBO). The inclusion of PEM instead of NCA reduces overall latency considerably. NCA uses a large set of complex functions, which is computationally extensive.On the contrary, PEM uses simple functions which require mild computation. Table 7 lists parameter values and shows the comparison for CHB-MIT scalp dataset. It is evident that this work enhances the current state of the art and contributes significantly to the smart healthcare system.

7 Conclusions

In this paper, a low-latency and low-power seizure detector has been presented. The proposed detector was extensively validated with both scalp EEG and intracranial icEEG databases. PEM with RBO effectively captures EEG dynamics, minimizes unused channels and features, and offers the best performance. The system's latency is reported as 1.05 sec, which is a 50-200% improvement in latency compared to the current state of the art. The active mode power consumption is recorded at 65.8 μw, which is useful for biomedical systems needing minimal power.

Potential future research is predicting seizures before their occurrence. The epilepsy patients' quality of life would improve if seizures could be properly predicted before they started and prevented with the appropriate measures. It is challenging to identify the preonset pattern, which would enable optimum detection accuracy because the preictal pattern differs for different epochs since the brain functioning varies from patient to patient. Another potential problem with healthcare devices is security. Healthcare devices and organizations possess important health and financial information and are vulnerable to cyberattacks. Hacker's access to healthcare data can put patients' privacy in danger. It can alter data on lifesaving devices and leads to devastating effects on the patients. Future research includes adding robust security with this detector to prevent devices from cyberattacks.

Acknowledgements This article is an expanded version of our prior conference paper that was presented at [25].

Compliance with Ethical Standards

The authors declare that they have no conflict of interest and there was no human or animal testing or participation involved in this research. All data were obtained from public domain sources.

References

1. S. P. Mohanty, U. Choppali, and E. Kougianos, "Everything You Wanted to Know about Smart Cities," *IEEE Consum. Electron. Mag.*, vol. 6, no. 3, pp. 60–70, July 2016.
2. A. Zanella, N. Bui, A. Castellani, L. Vangelista, and M. Zorzi, "Internet of Things for Smart Cities," *IEEE Internet Things J.*, vol. 1, no. 1, pp. 22–32, Feb 2014.
3. P. Sundaravadivel, E. Kougianos, S. P. Mohanty, and M. Ganapathiraju, "Everything You Wanted To Know About Smart Healthcare," *IEEE Consum. Electron. Mag.*, vol. 7, no. 1, pp. 18–28, Jan. 2018.
4. S. Kusmakar, C. K. Karmakar, B. Yan, T. J.O'Brien, R. Muthuganapathy, and M. Palaniswami, "Automated Detection of Convulsive Seizures Using a Wearable Accelerometer Device," *IEEE. Trans. Biomed. Eng.*, vol. 66, no. 2, pp. 421–432, Feb 2019.
5. N. Verma, A. Shoeb, J. Bohorquez, J. Dawson, J. Guttag, and A. P. Chandraksan, "A Micro-power EEG Acquisition SoC With Integrated Feature Extraction Processor for a Chronic Seizure Detection System," *IEEE J.Solid-State Circuits*, vol. 45, no. 4, pp. 804–816, April 2010.
6. B. J. Gluckman and C. Schevon, "Seizure Prediction 6: From Mechanisms to Engineered Interventions For Epilepsy," *Clin. Neurophysiol.*, vol. 32, no. 3, pp. 181–187, Jun 2015.
7. B. Direito, C. Teixeira, B. Ribeiro, M. Castelo-Branco, F. Sales, and A. Dourado, "Modeling Epileptic Brain States Using EEG Spectral Analysis And Topographic Mapping ," *J. Neurosci. Methods*, vol. 210, no. 2, pp. 220–229, Sep. 2012.
8. D. D. Spencer, J. L. Gerrard, and H. P. Zaveri, "The roles of surgery and technology in understanding focal epilepsy and its comorbidities," *Lancet Neurol.*, vol. 17, no. 4, pp. 373 – 382, 2018.
9. Y. Li, Y. Liu, W.-G. Cui, Y. Guo, H. Huang, and Z.-Y. Hu, "Epileptic Seizure Detection in EEG Signals Using a Unified Temporal-Spectral Squeezeand-Excitation Network," *IEEE Trans. Neural Syst. and Rehabil. Eng.*, vol. 28, no. 10, pp. 782–794, 2020.
10. L. A. Jones and R. H. Thomas, "Sudden death in epilepsy: Insights from the last 25 years ," *Seizure*, vol. 44, no. 3, pp. 232–236, Jan. 2017.
11. M. A. Sayeed, S. P. Mohanty, E. Kougianos, V. P. Yanambakha, and H. Zaveri, " A Robust and Fast Seizure Detection in IoT Edge ," in *Proc. IEEE Int. Symp. Smart Electron. Syst. (iSES)*, 2018, pp. 156–160.
12. A. Shoeb and J. Guttag, "Application of Machine Learning to Epileptic Seizure Detection," in *Proc. Int. Conf. on Machine Learning*, Haifa, Israel, 2010.
13. M. A. Sayeed, S. P. Mohanty, E. Kougianos, and H. P. Zaveri, "eSeiz: An Edge-Device for Accurate Seizure Detection for Smart Healthcare," *IEEE Trans. Consum. Electron.*, vol. 65, no. 3, pp. 379–387, 2019.
14. M. A. Sayeed, S. P. Mohanty, E. Kougianos, and H. Zaveri, "Neuro-Detect: A Machine Learning Based Fast and Accurate Seizure Detection System in the IoMT," *IEEE Trans. Consum. Electron.*, vol. 65, no. 3, pp. 359–368, 2019.
15. Z. Song, B. Deng, J. Wang, G. Yi, and W. Yue, "Epileptic seizure detection using brain-rhythmic recurrence biomarkers and onasnet-based transfer learning," *IEEE Trans. Neural Syst. and Rehabil. Eng.*, vol. 30, pp. 979–989, 2022.
16. Y. Guo, X. Jiang, L. Tao, L. Meng, C. Dai, X. Long, F. Wan, Y. Zhang, J. van Dijk, R. M. Aarts, W. Chen, and C. Chen, "Epileptic Seizure Detection by Cascading Isolation Forest-Based Anomaly Screening and EasyEnsemble," *IEEE Trans. Neural Syst. and Rehabil. Eng.*, vol. 30, pp. 915–924, 2022.
17. J.-L. Song, Q. Li, B. Zhang, M. B. Westover, and R. Zhang, "A New Neural Mass Model Driven Method and Its Application in Early Epileptic Seizure Detection," *IEEE. Trans. Biomed. Eng.*, vol. 67, no. 8, pp. 2194–2205, 2020.
18. M. Sahani, S. K. Rout, and P. K. Dash, "Epileptic Seizure Recognition Using Reduced Deep Convolutional Stack Autoencoder and Improved Kernel RVFLN From EEG

Signals," *IEEE Trans. Biomed. Circuits. Syst.*, vol. 15, no. 3, pp. 595–605, 2021.
19. X. Zhang, L. Yao, M. Dong, Z. Liu, Y. Zhang, and Y. Li, "Adversarial Representation Learning for Robust Patient-Independent Epileptic Seizure Detection," *IEEE J. Biomed. Health Inform.*, vol. 24, no. 10, pp. 2852–2859, 2020.
20. Y. S. Park, G. R. Cosgrove, J. R. Madsen, E. N. Eskandar, L. R. Hochberg, S. S. Cash, and W. Truccolo, "Early Detection of Human Epileptic Seizures Based on Intracortical Microelectrode Array Signals," *IEEE. Trans. Biomed. Eng.*, vol. 67, no. 3, pp. 817–831, 2020.
21. M. Geng, W. Zhou, G. Liu, C. Li, and Y. Zhang, "Epileptic Seizure Detection Based on Stockwell Transform and Bidirectional Long Short-Term Memory," *IEEE Trans. Neural Syst. and Rehabil. Eng.*, vol. 28, no. 3, pp. 573–580, 2020.
22. D. Wu, Z. Wang, L. Jiang, F. Dong, X. Wu, S. Wang, and Y. Ding, "Automatic Epileptic Seizures Joint Detection Algorithm Based on Improved Multi-Domain Feature of cEEG and Spike Feature of aEEG," *IEEE Access*, vol. 7, pp. 41 551–41 564, 2019.
23. O. Hanosh, R. Ansari, K. Younis, and A. E. Cetin, "Real-Time Epileptic Seizure Detection During Sleep Using Passive Infrared Sensors," *IEEE Sens. J.*, vol. 19, no. 15, pp. 6467–6476, 2019.
24. Y. R. Aldana, B. Hunyadi, E. J. M. Reyes, V. R. Rodríguez, and S. Van Huffel, "Nonconvulsive Epileptic Seizure Detection in Scalp EEG Using Multiway Data Analysis," *IEEE J. Biomed. Health Inform.*, vol. 23, no. 2, pp. 660–671, 2019.
25. M. A. Sayeed, S. Mohanty, E. Kougianos, and L. Rachakonda, "RSeiz: A Channel Selection Based Approach for Rapid Seizure Detection in the IoMT," in *IEEE Int. Symp. Smart Electron. Syst. (iSES)*, 2019, pp. 105–110.
26. W. Yang, K. Wang, and W. Zuo, "Neighborhood Component Feature Selection for High-Dimensional Data." *J. Comput.*, vol. 7, no. 1, Jan. 2012.
27. K. Najarian and R. Splinter, *Biomedical Signal and Image processing*. CRC Press, 2012, no. 9781439870334.
28. M. Robnik-Šikonja and I. Kononenko, "Theoretical and Empirical Analysis of ReliefF and RReliefF," *Machine Learning*, vol. 53, no. 1, pp. 23–69, Oct 2003.
29. R. J. Urbanowicz, M. Meeker, W. L. Cava, R. S. Olson, and J. H. Moore, "Relief-based Feature Selection: Introduction and Review," *J. Biomed. Inform*, vol. 85, pp. 189 – 203, 2018.
30. M. Robnik-Šikonja and I. Kononenko, "Theoretical and Empirical Analysis of ReliefF and RReliefF," *Machine Learning*, vol. 53, pp. 23–69, 2003.
31. I. Saini, D. Singh, and A. Khosla, "QRS Detection Using K-nearest Neighbor algorithm (KNN) and evaluation on standard ECG databases," *J. Adv. Res.*, vol. 4, no. 4, pp. 331–344, July 2013.
32. R. G. Andrzejak, K. Lehnertz, F. Mormann, C. Rieke, P. David, and C. E. Elger, "Indications of nonlinear deterministic and finite-dimensional structures in time series of brain electrical activity: Dependence on recording region and brain state," *Phys. Rev. E*, vol. 64, no. 6, p. 061907, Nov. 2001.
33. I. L. Olokodana, S. P. Mohanty, E. Kougianos, and O. O. Olokodana, "Real-Time Automatic Seizure Detection using Ordinary Kriging Method in an Edge-IoMT Computing Paradigm," *SN comput. sci.*, vol. 1, no. 5, 2020.
34. H. G. Daoud, A. M. Abdelhameed, and M. Bayoumi, "Automatic epileptic seizure detection based on empirical mode decomposition and deep neural network," in *Proc. IEEE Int. Conf. Signal Image Processing Appl. (CSPA)*, 2018, pp. 182–186.
35. T. W. T and Z. Zhang, "Effective and extensible feature extraction method using genetic algorithm-based frequency-domain feature search for epileptic EEG multiclassification," *Medicine*, vol. 96, no. 9, 2017.
36. A. L. Goldberger, "PhysioBank, PhysioToolkit, and PhysioNet: Components of a New Research Resource for Complex Physiologic Signals," *Circulation*, vol. 101, no. 23, pp. e215–e220, Jun. 2000.
37. L. S. Vidyaratne and K. M. Iftekharuddin, "Real-Time Epileptic Seizure Detection Using EEG," *IEEE Trans. Neural Syst. and Rehabil. Eng.*, vol. 25, no. 11, pp. 2146–2156, Nov 2017.
38. M. Fan and C. Chou, "Detecting Abnormal Pattern of Epileptic Seizures via Temporal Synchronization of EEG Signals," *IEEE. Trans. Biomed. Eng.*, vol. 66, no. 3, pp. 601–608, March 2019.
39. H. Peng, C. Li, J. Chao, T. Wang, C. Zhao, X. Huo, and B. Hu, "A Novel Automatic Classification Detection for Epileptic Seizure Based on Dictionary Learning and Sparse Representation," *Neurocomputing*, vol. 424, pp. 179–192, 2021.